Nanoscale

COMMUNICATION

View Article Online
View Journal | View Issue

Cite this: *Nanoscale*, 2018, **10**, 3650

Received 27th November 2017,
Accepted 22nd January 2018

DOI: 10.1039/c7nr08851e

rsc.li/nanoscale

What happens to the silver ions? – Silver thiocyanate nanoparticle formation in an artificial digestion†

Claudia Kästner,[a] Alfonso Lampen[b] and Andreas F. Thünemann*[a]

An artificial digestion of silver nitrate is reported. It is shown that AgSCN nanoparticles emerge from ionic silver in saliva and remain present during the entire digestion process. The particles were characterized by infrared spectroscopy and small- and wide-angle X-ray scattering (SAXS/WAXS) regarding their composition and size distribution.

Silver nanoparticles are attracting widespread interest due to their special properties.[1] Since silver shows antimicrobial behavior, its modification and synthesis as small nanoparticles for their application in medicine is constantly developed.[2] Simultaneously, silver nanoparticles have found their way into many consumer products ranging from textiles and cosmetics to water treatment and dietary supplements.[2–4] In contrast to gold, silver nanoparticles can continuously release ions through slow corrosion. For example, it was demonstrated by Sotiriou *et al.*[5] that small-sized silver nanoparticles (radius < 5 nm) release a significant concentration of silver ions from their surface. Therefore, biological impacts may emerge from formed silver ions and not from the nanoparticles themselves. Considering Sotiriou's study, it is reasonable to assume a co-existence of particle degradation and formation. Therefore, nanoparticle formation from silver ions has also to be taken into account.[6] Whereas most investigations focus on the incorporation of silver nanoparticles during digestion, only a small number of studies are dealing with the possible impact of a nanoparticle formation from silver ions in a physiological environment.

The major uptake route of silver particles and ions is oral ingestion.[7] The human digestion process includes different conditions which can strongly affect nanomaterials: wide pH shifts, high salt and enzyme concentrations, and an elevated temperature of 37 °C. Hence, for the evaluation of nanomaterials with regard to digestion, changes of their physicochemical properties including aggregation, interactions with biomolecules, and dissolution must be investigated under these conditions. These changes can strongly influence later biological effects of the nanoparticles (so-called "nano-effects"). Interconversions of the particles additionally indicate that a transition between ions and nanoparticles may play an important role. The group of Walczak[8] took a closer look at the impact of the digestive procedure on silver nitrate and its formed particles. They detected nanoparticles with radii of about 10–20 nm in the intestinal tract but not at the earlier stages of digestion. They also suggested the presence of smaller particles. This assumption lacks experimental proof due to the detection limit of single particle-inductively coupled plasma mass spectrometry (SP-ICPMS) of *ca.* 10 nm,[9] used in their study. They were not able to determine the composition of the formed nanoparticles unambiguously.

The aim of our study is therefore to enhance the knowledge of nanoparticle formation from silver nitrate during an artificial digestion. We used SAXS to monitor the emergence of particles and changes in their size distribution. SAXS allows *in situ* detection of particles with radii of 0.5 to 50 nm in complex media, such as digestive juices. We adapted a standardized digestion procedure consisting of three main steps: saliva, stomach and intestine (Fig. 1).[10,11] These steps include pH shifts, transit times and the typical digestive juices consisting of salts and enzymes. Additionally, also the behavior of silver nitrate in the presence of a mixture of relevant food components[11] (oil, starch and skimmed milk powder) was studied to simulate a realistic surrounding present at oral uptake. The samples were analyzed with SAXS after every step.

The SAXS curves from saliva, stomach and intestine are typical for the presence of nanoparticles, which are not visible in the undigested silver nitrate solution (see Fig. 1). Volume-weighted radii distributions were evaluated with a Monte Carlo based data evaluation procedure[12] which was proven suitable for precise nanoparticle size distribution quantification.[13] The resulting size distributions are shown in Fig. 2. Defined nano-

[a]*Bundesanstalt für Materialforschung und -prüfung (BAM), Unter den Eichen 87, 12205 Berlin, Germany. E-mail: andreas.thuenemann@bam.de*
[b]*Bundesinstitut für Risikobewertung (BfR), Max-Dohrn-Straße 8-10, 10589 Berlin, Germany*

† Electronic supplementary information (ESI) available: Details of the materials and methods and SAXS/WAXS data. See DOI: 10.1039/c7nr08851e

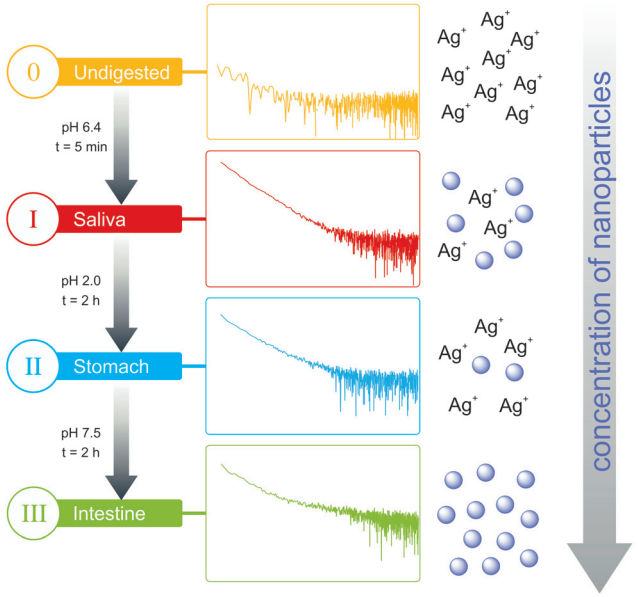

Fig. 1 Scheme of the artificial digestion, the formation of nanoparticles, and monitoring by SAXS with the corresponding curves. Displayed are the 4 steps of the procedure (before digestion, saliva, stomach, and intestine).

particle populations are present at all steps of digestion. The distributions are bimodal with particles with radii R_1 < 5 nm and particles with radii R_2 > 5 nm. Maxima for the small particles are clearly visible in the range of 2–4 nm, while no clear maxima are present for the larger particles. For quantification, the distributions were fitted by a sum of two cumulative log-normal functions which consist of two contributions:

$$F(R) = \frac{a_1}{2}\mathrm{erfc}\left(\frac{\log\left(\frac{R_{0,1}}{R}\right)}{\sqrt{2}w_1}\right) + \frac{a_2}{2}\mathrm{erfc}\left(\frac{\left(\log\left(\frac{R_{0,2}}{R}\right)\right)}{\sqrt{2}w_2}\right)$$

a_i are scaling factors which correlate with the volume fraction of the small and larger particles, respectively. $R_{0,i}$ are the median radii and w_i are width parameters of the distribution. The mean radii R_i and the relative widths of the size distributions σ_i were calculated as

$$R_i = R_{0,i}e^{\frac{w_i^2}{2}} \text{ and } \sigma_i = R_i\sqrt{e^{2w_i^2} - e^{w_i^2}}.$$

Since the SAXS measurements are defined on an absolute scale, the overall conversion of the silver ions into nanoparticles can be determined with the help of the resultant volume fraction and the density of the nanoparticles (ρ = 3.828 g cm^{-3}, AgSCN).[14]

The experiments started with the digestion of silver nitrate in the absence of food components. Already in saliva, nanoparticles are formed (Fig. 2a). At this stage, the particles were incubated in saliva for 5 min at 37 °C. The formed particle system consists of small particles with a narrow distribution

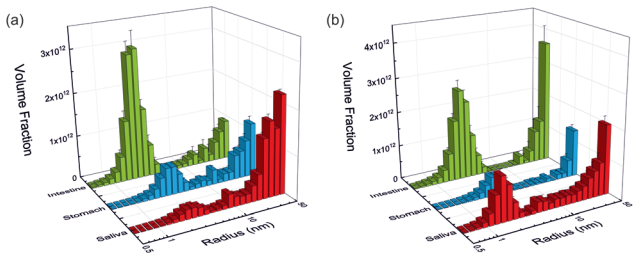

Fig. 2 Volume-weighted size distributions derived by SAXS measurements of nanoparticles formed from (a) silver nitrate and (b) silver nitrate in the presence of food components at the three digestion steps: saliva, stomach and intestine (red, blue and green bars, respectively).

width and larger particles which display a broader size distribution. A mean volume-weighted radius of R_1 = 4.0 ± 0.6 nm and a distribution width of σ_1 = 1.4 nm were determined for the small particles. All size distribution characteristics of the nanoparticles are summarized in Table 1. The small and large particles have relative volume fractions of 18% and 82%, respectively (Fig. 3c), and the overall yield of the conversion of silver ions into particles amounts to 79%. The following steps of digestion are the artificial gastric tract which includes a pH shift to a value of 2, with an incubation time of 2 h at 37 °C, and the intestine with a pH shift to 7.5 (incubation time and temperature are identical to stomach). During these digestion steps, the fraction of small particles increases in the stomach to 48% and finally in the intestine to 78%. The small particles' radius is decreasing at the same time from 3.3 ± 0.2 nm to 2.0 ± 0.1 nm in the intestinal tract. We also observed that the larger particles, which are present during every step, are also decreasing in size from 45 ± 6 nm in saliva to 30 ± 2 nm in the intestine. The yield of the conversion decreases in the stomach to 52%, whereas in the intestine, a full conversion of 100% was determined. We conclude that the digestive process promotes the formation of new particles. In particular, the small particles show a narrowing size distribution with distribution

Table 1 Size distribution parameters of nanoparticles resulting from the digestion of $AgNO_3$ and $AgNO_3$ + food components (starch, oil and skimmed milk powder): small particle radii R_1, their distribution width σ_1, their relative volume fraction and radii of large particles R_2, their distribution width σ_2 and the overall yield of the conversion of silver ions into particles. Volume fractions of large particles can be calculated by: 100% – volume fraction of small particles

Sample	R_1 (nm)	σ_1 (nm)	Fraction (%)	R_2 (nm)	σ_2 (nm)	Yield (%)
Saliva						
$AgNO_3$	4.0 ± 0.6	1.4	18 ± 2	45 ± 6	11	79
$AgNO_3$ + food	1.7 ± 0.1	0.3	45 ± 2	29 ± 2	8	89
Stomach						
$AgNO_3$	3.3 ± 0.2	0.8	48 ± 1	32 ± 1	4	52
$AgNO_3$ + food	3.0 ± 0.1	0.5	53 ± 1	39 ± 1	2	34
Intestine						
$AgNO_3$	2.0 ± 0.1	0.2	78 ± 1	30 ± 2	6	100
$AgNO_3$ + food	2.3 ± 0.1	0.3	62 ± 1	38 ± 1	3	100

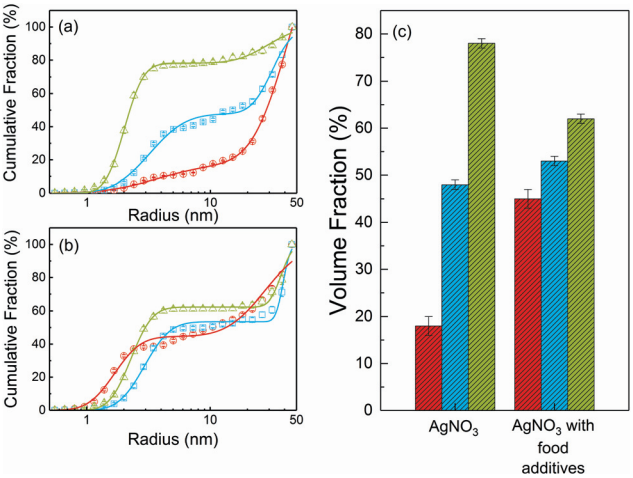

Fig. 3 (a) and (b) Volume-weighted size distributions in cumulative fraction presentation at the three stages: saliva, stomach and intestine (red, blue and green symbols, respectively) with their corresponding fit curves (solid lines). Displayed are the resulting particles of the digestion of $AgNO_3$ (a) and $AgNO_3$ in the presence of food components (b). (c) Relative volume fractions of small particles at the three digestive steps.

widths of 1.4 nm, 0.8 nm and 0.2 nm, respectively (saliva, stomach and intestine). The radii of small and larger particles are decreasing in the course of digestion (Fig. 4). A possible reason is the increasing amount of potentially stabilizing proteins in the digestive fluids, which enables a particle formation even in the first step of saliva.

As mentioned above, Walczak *et al.*[8] observed the formation of nanoparticles only in the intestinal tract, which is not in contrast to our results. The apparent differences between their and our results are due to the different lower detection limits of SP-ICPMS ($R_{limit} \geq 10$ nm) and SAXS ($R_{limit} \geq 0.5$ nm). We assume that the particles they found in the intestine are identical to the larger particles observed in our study. In addition to their findings, we could prove that nanoparticles in the sub 10 nm range are present at each step of the digestive process.

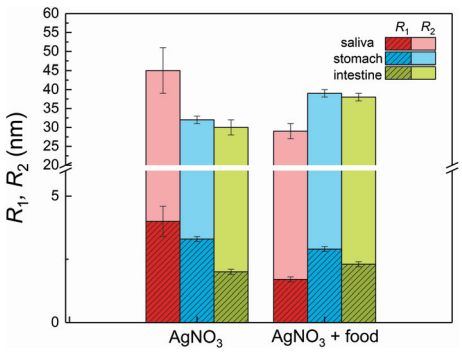

Fig. 4 Mean volume-weighted radii of the small particles R_1 and of the larger particles R_2 formed during the digestion of $AgNO_3$ and $AgNO_3$ in the presence of food components. The radii are displayed according to the digestion steps: saliva, stomach and intestine (red, blue and green bars, respectively).

The course of digestion of silver nitrate in the presence of a mixture of food components is depicted in Fig. 2b and 3b. Obviously, the formation of nanoparticles with radii lower than 5 nm starts also in saliva. Again, the size distribution is bimodal and contains small and larger particles. Here, the mean radius of the small particles is 1.7 ± 0.1 nm, whereas the larger ones show a mean radius of 29 ± 2 nm. The volume fraction of the small particles is 45%. The radii of small and large particles are reduced in comparison with the experiment without food components. The volume fraction of the small particles is twice as high as before. In a recent study about the digestion of silver nanoparticles, we observed that food components improve colloidal stability of the particles during digestion.[11] Therefore, we assume that a stabilizing effect may also be present for nanoparticles produced from silver nitrate in saliva. The further steps of digestion show an increase in the volume fraction of small particles to 53% and 62% for the gastric and intestinal tract, respectively. The corresponding mean radii are 3.0 ± 0.1 nm in the stomach and 2.3 ± 0.1 nm in the intestine. Simultaneously, the radii of the larger particles increase in the gastric tract to 39 ± 1 nm. This value remains constant until the end of digestion (38 ± 1 nm in the intestine). The characteristics of the small particles in the stomach are not significantly different for the digestion with or without food components. This indicates that the food components provide only a minor stabilizing effect on the formed particles in stomach and intestine. Also the characteristics of the larger particles are independent of the presence of food components after passing the stomach and intestine (Fig. 4). The variation of the yield for the conversion of silver ions to particles shows the same trend as without food components: in saliva, a high yield of 89% is observed, whereas this decreases to 34% in the stomach. In the intestine, a full conversion is determined.

The composition of the particles remains an open question. The assumption of Walczak *et al.*, that their particles consist of AgCl and Ag_2S, is based on energy dispersive X-ray spectroscopy (EDX) data. The EDX signals corresponded to silver, sulphur and chlorine species located at and nearby the particles. These findings need to be interpreted with caution since EDX provides only information on the elements located within the measured area. The electron beam cannot be focused on a single particle and, therefore, includes also signals of the surrounding environment. To elucidate the composition of the formed nanoparticles, we measured WAXS of the formed particles in order to reveal their crystalline structure. Unfortunately, the reflections of nanoparticles are very broad which often prevents an assignment of the crystal structure. Nevertheless, we can exclude the presence of AgCl and Ag_2S by direct comparison of the WAXS curve of the particles with those of suitable silver salts (AgCl, Ag_2S, Ag_2SO_4, Ag_3PO_4, and AgSCN; see ESI, Fig. S3†). Additionally, the off-white color of the particles proves that they cannot consist of Ag_2S (dark brown colored). Hence, also oxides can be excluded because of their black color. Silver hydroxides are formed only at basic pH values and can be ruled out because the pH value ranged between 2.0 and 7.5 in the artificial digestion. Bare silver clus-

ters can also be excluded because of the absence of their typical plasmon resonance band at *ca.* 400 nm. Instead, the WAXS signal is indicative of AgSCN and we used IR spectroscopy to verify this assumption. The particles show two strong absorbance maxima at 2086 cm^{-1} and 2102 cm^{-1} as shown in Fig. 5. As control, the saliva without added silver nitrate (labeled saliva blank) was measured and shows no bands in this region. IR signals at wavenumbers in the range of 2100 cm^{-1} are significant for thiocyanate compounds.[15] Therefore, we also measured pure silver thiocyanate which shows the same absorbance maxima as our particles. From combining WAXS and IR results, we conclude that the particles are composed of silver thiocyanate. In water, AgSCN has a solubility of 1.68×10^{-4} g L^{-1} which is the lowest of the suitable silver salts. Therefore, we speculate that the AgSCN nanoparticle formation is thermodynamically driven.

This finding is not in contradiction with the results of Walczak *et al.* since the sulphur EDX signal is in line with the presence of AgSCN nanoparticles. Among the rare literature studies about AgSCN nanoparticles are the synthesis by Yang and Ma[16] using AgCl as a precursor and by Zurmühl *et al.*[17] who used a microemulsion process.

In summary, we investigated an artificial digestion of silver nitrate monitored by SAXS and complemented it with WAXS and IR spectroscopy. We were able to demonstrate that silver thiocyanate nanoparticles were formed in saliva and through the entire digestion. It is, to the best of our knowledge, the first study to characterize these emergent particles directly in digestive media. The particles reveal a bimodal size distribution. Surprisingly, the small particles with mean radii in the range of 1.5–4 nm display a narrow size distribution, whereas the large particles show broad size distributions with mean radii of 30–50 nm. The addition of typical food components does not alter the results significantly, except in saliva. These results may have an impact on the conception of biological studies dealing with silver based materials.

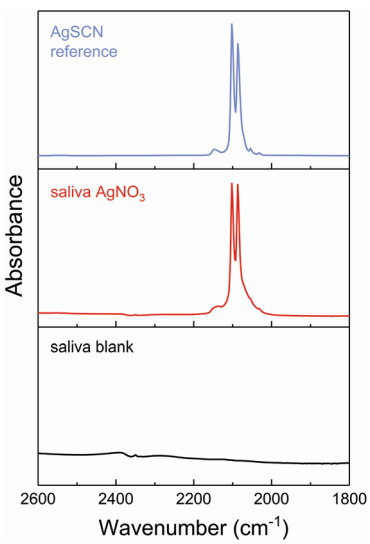

Fig. 5 IR spectra of particles formed from $AgNO_3$ in saliva, control saliva (without particles/$AgNO_3$) and pure AgSCN (red, black and purple solid lines, respectively). Strong absorption bands of AgSCN are found at 2102 cm^{-1} and 2086 cm^{-1}.

Conflicts of interest

There are no conflicts of interest to declare.

Acknowledgements

We thank Maximilian Ebisch and Petra Fengler for their help in performing the artificial digestion. We also thank H. V. Schröder and P. E. J. Saloga for thorough discussion of the manuscript.

References

1 S. Chernousova and M. Epple, *Angew. Chem., Int. Ed.*, 2013, **52**, 1636–1653.
2 S. Chernousova and M. Epple, *Angew. Chem., Int. Ed.*, 2013, **52**, 1636–1653.
3 L. Windler, M. Height and B. Nowack, *Environ. Int.*, 2013, **53**, 62–73.
4 M. E. Vance, T. Kuiken, E. P. Vejerano, S. P. McGinnis, M. F. Hochella Jr., D. Rejeski and M. S. Hull, *Beilstein J. Nanotechnol.*, 2015, **6**, 1769–1780.
5 G. A. Sotiriou and S. E. Pratsinis, *Curr. Opin. Chem. Eng.*, 2011, **1**, 3–10.
6 R. D. Glover, J. M. Miller and J. E. Hutchison, *ACS Nano*, 2011, **5**, 8950–8957.
7 S. W. P. Wijnhoven, W. J. G. M. Peijnenburg, C. A. Herberts, W. I. Hagens, A. G. Oomen, E. H. W. Heugens, B. Roszek, J. Bisschops, I. Gosens, D. Van De Meent, S. Dekkers, W. H. De Jong, M. van Zijverden, A. J. A. M. Sips and R. E. Geertsma, *Nanotoxicology*, 2009, **3**, 109–138.
8 A. P. Walczak, R. Fokkink, R. Peters, P. Tromp, Z. E. Herrera Rivera, I. M. C. M. Rietjens, P. J. M. Hendriksen and H. Bouwmeester, *Nanotoxicology*, 2012, **7**, 1198–1210.
9 A. R. Montoro Bustos, E. J. Petersen, A. Possolo and M. R. Winchester, *Anal. Chem.*, 2015, **87**, 8809–8817.
10 D. 19738, *Journal*, 2004-07.
11 C. Kästner, D. Lichtenstein, A. Lampen and A. F. Thünemann, *Colloids Surf., A*, 2017, **526**, 76–81.
12 I. Bressler, B. R. Pauw and A. F. Thünemann, *J. Appl. Crystallogr.*, 2015, **48**, 962–969.
13 B. R. Pauw, C. Kästner and A. F. Thünemann, *J. Appl. Crystallogr.*, 2017, **50**, 1280–1288.
14 H.-L. Zhu, G.-F. Liu and F.-J. Meng, *Z. Kristallogr. – New Cryst. Struct.*, 2003, **218**, 263–264.
15 D. B. Parry, J. M. Harris and K. Ashley, *Langmuir*, 1990, **6**, 209–217.
16 M. Yang and J. Ma, *Appl. Surf. Sci.*, 2009, **255**, 9323–9326.
17 C. Zurmühl, S. Wolf and C. Feldmann, *Z. Anorg. Allg. Chem*, 2015, **641**, 1510–1514.